

Available online at [www.sciencedirect.com](http://www.sciencedirect.com)**ScienceDirect**

Procedia Engineering 140 (2016) 1 – 7

**Procedia  
Engineering**[www.elsevier.com/locate/procedia](http://www.elsevier.com/locate/procedia)**RS Singapore – ICMAT Symposia Proceedings**

8th International Conference on Materials for Advanced Technologies

**A Novel Photonic Crystal Fiber Biosensor Using Surface Plasmon Resonance**

A. A. Rifat\*, G. Amouzad Mahdiraji, Y. G. Shee, Md. Jubayer Shawon, F. R. Mahamd Adikan

*Integrated Lightwave Research Group, Department of Electrical Engineering, Faculty of Engineering, University of Malaya, Kuala Lumpur-50603, Malaysia***Abstract**

A novel photonic crystal fiber (PCF) biosensor based on surface plasmon resonance (SPR) phenomena is proposed. Chemically stable active plasmonic material gold (Au) and sensing layer is used outside the fiber structure to make the sensor configuration simpler. The proposed sensor would be able to detect the unknown analytes by flowing through the metal surface or dripped on the outer surface of the metal layer. The proposed sensor is consist with the symmetrical circular air-holes. Two small air-holes are used in the second rings which helps to produce the more evanescent field as well as helps to tune the phase matching between the core guided mode and surface plasmon polaritons (SPP) mode. Surface plasmons along the metal surface is excited with the leaky Gaussian-like core guided mode. Guiding properties and the sensing performance are numerically investigated by the Finite Element Method (FEM). A circular, perfectly matched layer is used to absorb the radiation towards the surface. Using the wavelength interrogation mode, proposed sensor shows the maximum sensitivity of 1,000 nm/RIU (Refractive Index Unit), with the sensor resolution as low as  $1 \times 10^{-4}$  RIU. The proposed sensor design shows the promising results that could be used in biological and biochemical analytes detection.

© 2016 The Authors. Published by Elsevier Ltd. This is an open access article under the CC BY-NC-ND license (<http://creativecommons.org/licenses/by-nc-nd/4.0/>).

Selection and/or peer-review under responsibility of the scientific committee of Symposium 2015 ICMAT

*Keywords:* Surface Plasmon Resonance; Plasmonic; Photonic Crystal Fiber; Fiber Opticas Sensors.

## 1. Introduction

Surface plasmon resonance sensors have shown the much attention since last few decades because of its extremely sensitive performance. Generally the commercial prism coupled geometry is used for the SPR sensors. Prism is used to pass the light to the metal surface interface, whereas transverse magnetic (TM) or p-polarized light is induced in the metal or dielectric interface. The incident light is absorbed by the free electrons of the metal surface as a result, surface plasmon wave (SPW) is generated. The prism based SPR sensor is bulky and its limit the remote sensing applications [1, 2]. To overcome those problems, photonic crystal fiber based SPR sensor is introduced. PCF is small in size and has design flexibility. Based on the applications, core-guided leaky-mode propagation can be controlled by using different types of PCF's structures such as hexagonal, square, octagonal, decagonal, hybrid, etc.; and also guiding can be controlled by optimizing the structural parameters [3, 4]. The guided light of the optical fiber is modified by the external agents (due to physical, chemical or biological effects) and could be detected from the output light. PCF SPR sensors are work based on the evanescent field which is produced due to the light propagation through the core-cladding region. The evanescent tails of the surface plasmon light interact with the plasmonic surface. Therefore, the refractive index of the guided light will change. Due to change of the analyte refractive index (RI), the vicinity surface real part of the effective index of the surface plasmon polaritons (SPP) will change, as a result phase matching point or resonant wavelength also change. The particles or molecules are detected by measuring this resonant wavelength shifting. This is the basic working principle of the PCF SPR sensors [5, 6].

In 1993, first optical fiber based SPR sensor has been proposed by R.C. Jorgenson where, the fiber core was coated with the gold film by removing a section of the fiber cladding to exhibit the plasmonic response [7]. Being a SPR sensor, phase matching condition should to be satisfied; whereas the core guided fundamental mode, surface plasmon polaritons (SPP) mode and propagation loss peak will match at a certain wavelength. At that phase matching wavelength, unknown analyte will be detected by shifting the resonance peak. M. A. Schmidt *et al.* introduced the fabrication of gold nanowire with photonic crystal fiber and observed the SPR phenomenon experimentally for the first time [8]. Polymer based selectively coated PCF structure is proposed by Jitendra Narayan Das and Rajan Jha to investigate the sensing performance in the near infrared wavelength [9]. Selectively infiltrated of the analyte-core is introduced to exhibit the coexistence of positive and negative refractive index sensitivity [10]. Moreover, multiple graphene layer also introduced with the birefringence control PCF structure for the SPR sensor by Jitendra Narayan Das and Rajan Jha [11]. Selectively deposition of metal into the fiber holes and also selectively infiltrated the liquid or analytes are challenging. High pressure chemical vapour deposition (CVD) technique is reported by Sazio *et al.* to homogeneously coat the metal in the fiber air holes or core [12]. Most of the reported PCF SPR sensors are used the multiple metal layer and liquid infiltration inside the air-holes, which is difficult in terms of fabrication. Recently, PCF SPR biosensors realized by keeping the metallic layer and sensing layer outside the PCF structure has been proposed where the different air-hole sizes are introduced and placed at different positions to control the light propagation in specific directions [13, 14]. Nonetheless, fabrication of such irregular PCF geometry is difficult even with very accurate fiber preform drilling systems.

Generally, gold and silver metal is widely used as an active plasmonic material. Silver is a most conductive material. Its resonance peak is very sharp also it shows the higher detection accuracy compared to gold [6]. However, silver is oxidized easily which reduced the detection accuracy, consequently, sensor performance also hampered. To prevent the silver oxidation graphene layer is used in this work. Graphene stop the oxygen molecules to pass through it, as a result silver will not be oxidized [15]. As an alternative plasmonic material, Gold is chemically stable even in aqueous environment. Moreover, it shows the larger wavelength shift at the resonant wavelength which helps for the easy detection and increase the accuracy to detect the unknown analyte accurately [14].

In this paper, we introduced a practically simple, regular hexagonal PCF SPR biosensor where the gold and sensing layer are placed outside the fiber structure which helps to reduce the design complexity and make the sensing process

simpler. Unknown analyte detection can be carried out by flowing the analyte or just placing the analyte outside the gold surface. Our proposed sensor is simpler compared to the reported PCF SPR sensors, in terms of fabrication.

## 2. Structural Design & Numerical Analysis

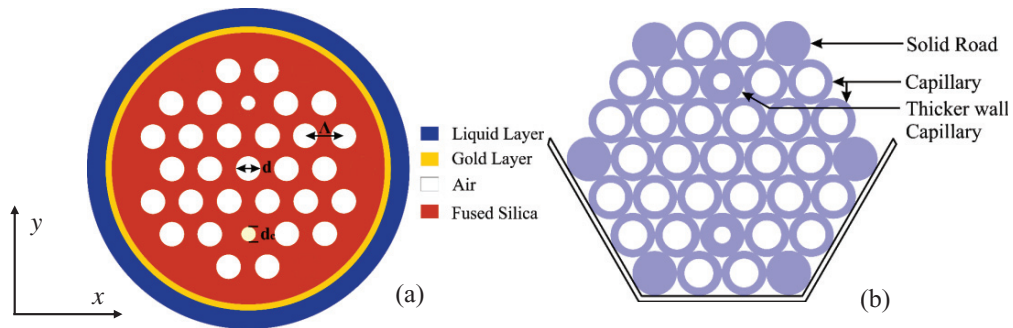


Fig. 1 (a) Cross-section of the proposed sensor; (b) Cross-section of the proposed PCF's stacked preform.

Fig. 1 (a) shows the cross-section of the proposed sensor. A simple 3 ring, hexagonal PCF structure is introduced for the SPR sensor. Two small air-holes are used along the central air-hole. Besides the small air-holes, two opposite holes are omitted to make a gap for the evanescent field flow to excite the metal surface. By introducing the thicker wall capillaries and solid rods, proposed PCF's can be fabricated, as shown in Fig. 2(b). By following the standard fiber drawing Stack-and-Draw method proposed PCF can be fabricated. Due to small air-holes there has large silica surface which will act as a core and propagate the light following the total internal reflection (TIR) method. Proposed sensor structural parameters pitch size,  $\Lambda = 1.70 \mu\text{m}$ , air hole diameter,  $d = 0.5\Lambda$  and the core diameter,  $d_c = 0.25\Lambda$  is used. Moreover, the gold thickness is considered 40 nm in the ideal case and the dielectric constant of gold has been taken by following the Drude-Lorentz model [14]. Additionally, refractive index of Silica has been taken using the Sellmeier equation [13].

$$n^2(\lambda) = 1 + \frac{B_1\lambda^2}{\lambda^2 - C_1} - \frac{B_2\lambda^2}{\lambda^2 - C_2} - \frac{B_3\lambda^2}{\lambda^2 - C_3} \quad (1)$$

where, refractive index of silica is  $n$  and  $\lambda$  is wavelength in  $\mu\text{m}$ . Moreover, Sellmeier coefficients,  $B_1 = 0.69616300$ ,  $B_2 = 0.407942600$ ,  $B_3 = 0.897479400$ ,  $C_1 = 4.67914826 \times 10^{-3} \mu\text{m}^2$ ,  $C_2 = 1.35120631 \times 10^{-2} \mu\text{m}^2$  and  $C_3 = 97.9340025 \mu\text{m}^2$ .

We employ the finite-element method with the good radiation absorber perfectly matched layer boundary condition on the outmost layer and also the scattering boundary condition is used on the outer surface to investigate the mode confinement.

## 3. Results and Discussion

PCF SPR sensor work based on the evanescent fields. Efficient excitation of the metal surface is a key factor of plasmonic phenomenon. At a certain wavelength, incident field can excite the surface and generate the resonance. In the proposed sensor, two small-holes has significant influence on the phase matching behaviour. The small holes size has been fixed with  $d_c = 0.25\Lambda$ , if the diameter is reduced than this, light will more concentrate through the core but, for the SPR phenomena surface excitation is an important issue. Moreover, if increase the small air-holes diameter

then the core guided effective index will be reduced and the guiding light will spread out over the cladding region resulting the surface excitation will be reduced. In this work, x-polarization fundamental mode has been considered, due to its high modal loss compare to the x-polarization. Moreover, y-polarization produced evanescent field and surface excitation is less compared to the x-polarization component. The fundamental core-guided mode, surface plasmon polaritons (SPP) mode and the phase matching mode are shown in Fig. 2.

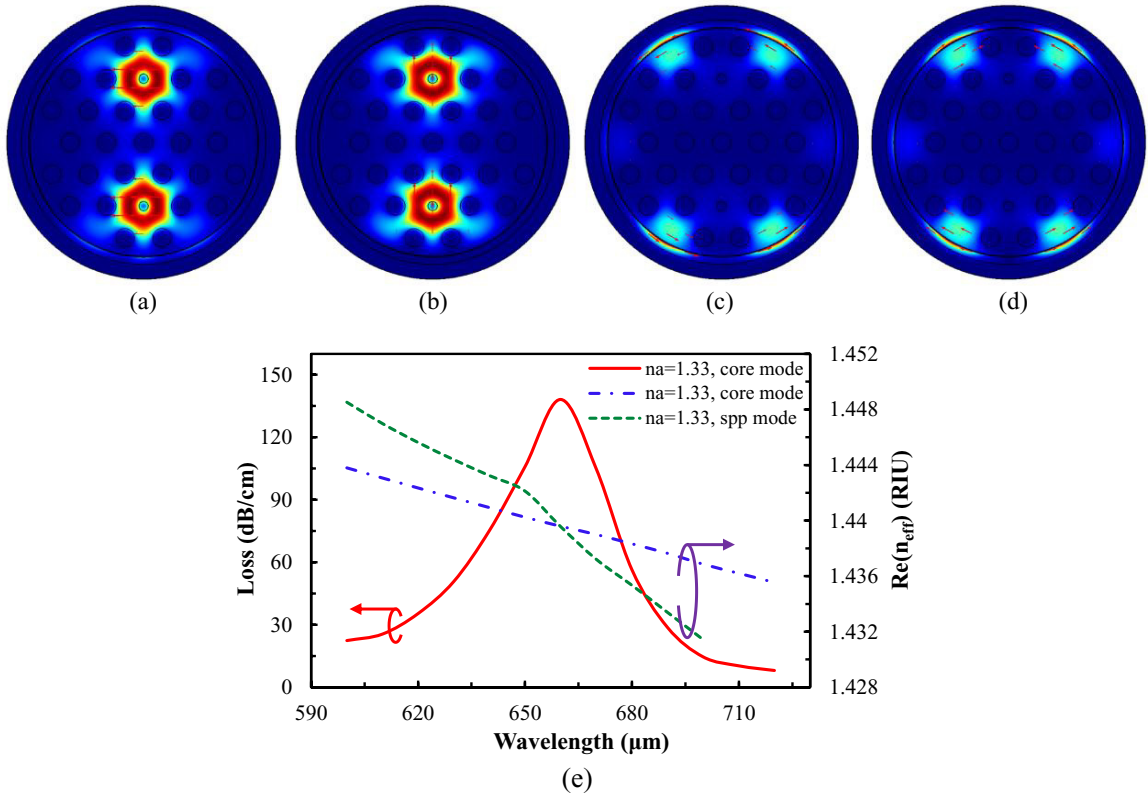


Fig. 2 Field profiles of Core-guided mode (a) and (b) for x-polarization and y-polarization, respectively; (c) and (d) SPP mode for x-polarization and y-polarization, respectively. (e) Dispersion relation of core-guided mode and SPP mode.

Fig. 2(a) and (b) shows the electric field profile of the fundamental core-guided mode for x-polarization and y-polarization, respectively and 2(c) and (d) shows the SPP mode for x-polarization and y-polarization, respectively. The real part of the fundamental mode and the SPP mode are presented by the blue and green solid line, respectively. The modal loss of the fundamental core guided mode is calculated by the following equation [16].

$$\alpha = 40\pi \cdot \text{Im}(n_{\text{eff}}) / (\ln(10)\lambda) \approx 8.686 \times k_0 \cdot \text{Im}[n_{\text{eff}}] \times 10^4 \text{ dB/cm} \quad (2)$$

where,  $k_0 = 2\pi/\lambda$  is the wave number in the free space and the wavelength,  $\lambda$  is in  $\mu\text{m}$ . At the wavelength 660 nm, a very sharp loss peak is found also the effective index of core guided fundamental mode and SPP mode are coincide together; it indicates the maximum power transfer from the core guided mode to the SPP mode. The loss peak is found due to the core-cladding refractive index contrast. Without influenced by the higher order plasmonic modes, it shows the one resonance peak for the fundamental mode. The presence of the resonance on the metal surface indicates the sensing performance. Fig. 2(a) shows the phase matching phenomena where fundamental core mode, SPP mode and the loss peak are well-matched at a given wavelength 660 nm. Additionally, Fig. 2(c) shows the electric field is

introduced on the metal surface outside the resonant wavelength. Proposed sensor is very sensitive with respect to the analyte refractive index. By varying the analyte refractive index (RI) from 1.33 to 1.37 is shown in Fig. 3.

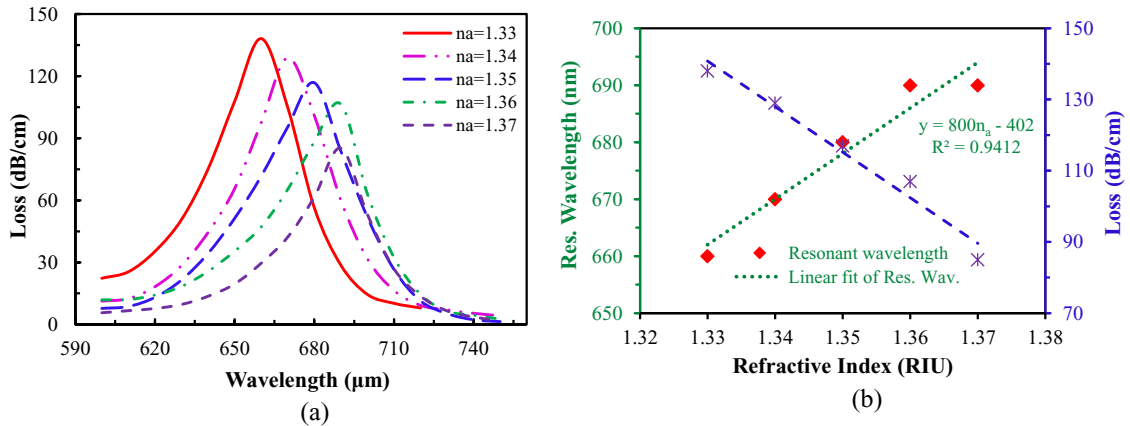


Fig. 3 (a) Loss spectrum of the proposed sensor by varying the analyte RI from 1.33 to 1.37; (b) Linear fit curve of the proposed sensor.

As it stated in Fig. 3(a), with the increasing of analyte RI, peak loss spectrum are moves towards the longer wavelength. Also, the amplitude of the loss spectrums are decreases gradually with the increasing of analyte RI. To detect the analytes, wavelength interrogation method and the amplitude (phase) detection methods are much familiar. The wavelength interrogation method shows the higher sensitivity and the higher detection range compare to the amplitude detection method [6]. By following the wavelength interrogation method, while analyte refractive index is changed from 1.33 to 1.37, a maximum positive RI sensitivity 1000 nm/RIU is achieved which is comparable with ref. [9]. Maximum amplitude of the loss spectrum 138 dB/cm is found at wavelength 660 nm for analyte refractive index,  $n_a=1.33$  and for the analyte RI  $n_a=1.37$ , the loss depth decrease to 85 dB/cm at 690 nm wavelength.

Wavelength interrogation sensitivity is define as [6], Sensitivity,  $S_\lambda(\text{nm}/\text{RIU}) = \Delta\lambda_{\text{peak}}/\Delta n_a$ , where  $\Delta\lambda_{\text{peak}}$  is the resonance peak shift and  $\Delta n_a$  is the variation of the analyte refractive index. Moreover, the resonant peaks are found at the wavelength 670, 680 and 690 nm for the analyte RI 1.34, 1.35 and 1.36, respectively shown in Fig. 3(b). Fig. 3(b) indicates the sensor performance consistency in the sensing range 1.33 to 1.37. The linear resonant wavelength shift where linear regression  $R^2$  is 1, which is a good signature of high linearity. Proposed sensor shows the constant sensitivity of 1000 nm/RIU while the analyte RI varied from 1.33 to 1.36 with the iteration 0.01. However, only the higher sensitivity does not indicate a good sensor, also precisely detect the small change of the spectral shift is important to detect the analytes accurately. By the performance of sensor resolution, it is possible to accurately measure the small change of the spectral shift. The proposed sensor maximum peak shift is  $\Delta\lambda_{\text{peak}}=10$  nm and the analyte RI changes  $\Delta n_a=0.01$  according to Fig. 3(a). If we assume proposed sensor can accurately detect the  $\Delta\lambda_{\text{min}}=0.1$  spectral resolution. So, the proposed sensor resolution is  $1 \times 10^{-4}$  RIU which is calculated by, Resolution,  $R = \Delta n_a \times \Delta\lambda_{\text{min}} / \Delta\lambda_{\text{peak}}$  RIU; and our result is comparable with the ref. [9].

Furthermore, the amplitude detection method or the phase detection method is very modest and also cost effective to measure the sensitivity. Spectral manipulation is not necessary in this method [6]. By changing the analyte RI amplitude sensitivity is shown in Fig. 4. According to Fig. 4, maximum amplitude sensitivity is achieved 118 RIU<sup>-1</sup> for the analyte refractive index 1.33.

The amplitude sensitivity can be obtained by the following equation [6]:

$$S_A(\lambda)[\text{RIU}^{-1}] = -\frac{1}{\alpha(\lambda, n_a)} \frac{\partial \alpha(\lambda, n_a)}{\partial n_a} \quad (3)$$

Here,  $\alpha(\lambda, n_a)$  is the overall propagation loss along the wavelength at a specific analyte refractive index and  $\partial\alpha(\lambda, n_a)$  is the difference between the loss spectra, before and after the analyte refractive index change.

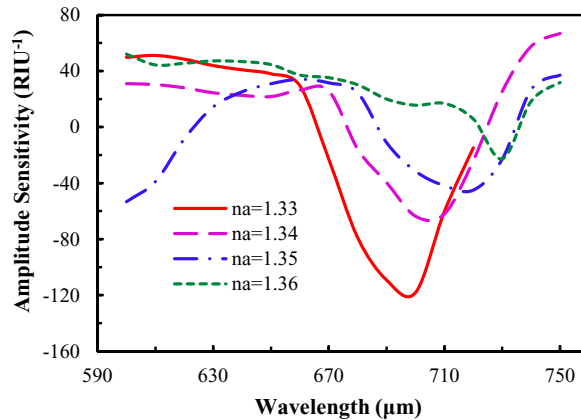


Fig. 4 Amplitude sensitivity as a function of wavelength with varying analyte RI  $n_a$  1.33 to 1.36.

According to Fig. 4, amplitude sensitivities are found 118, 64, 45 and 23  $\text{RIU}^{-1}$  for the analyte RI 1.33, 1.34, 1.35 and 1.36, respectively. The highest sensitivity is shown 118  $\text{RIU}^{-1}$  at 700 nm wavelength. If we assume, for the 1% change in the transmitted intensity can be sensed accurately, as a result, the sensor resolution will be  $8.5 \times 10^{-5}$  RIU.

#### 4. Conclusion

In this work, we numerically investigate the photonic crystal fiber surface plasmon resonance biosensor. Full-vectorial Finite-element method is used to explore the guiding properties. To abolish the radiation towards the surface, a circular perfectly matched layer is used. Proposed sensor shows the wavelength and amplitude sensitivities of 1000 nm/RIU and 118  $\text{RIU}^{-1}$ , respectively. Additionally, proposed sensor shows the sensor resolution  $1 \times 10^{-4}$  RIU and  $8.5 \times 10^{-5}$  RIU, considering the wavelength and amplitude interrogation method. Due to the promising results and simple sensing scheme, proposed sensor could be a potential candidate for biological and biochemical analytes detection.

#### Acknowledgment

This work is fully supported by the University of Malaya, MOHE-High Impact Research grant No. UM.000005/HIR.C1.

#### References

- [1] B. Gupta and R. Verma, "Surface plasmon resonance-based fiber optic sensors: principle, probe designs, and some applications," *J. Sens.*, vol. 2009, 2009.
- [2] J. Homola, S. S. Yee, and G. Gauglitz, "Surface plasmon resonance sensors: review," *Sens. Actuat. B Chem.*, vol. 54, pp. 3-15, 1999.
- [3] R. Ahmmed, R. Ahmed, and S. A. Razzak, "Design of large negative dispersion and modal analysis for hexagonal, square, FCC and BCC photonic crystal fibers," in *Informatics, Electronics & Vision (ICIEV)*, 2013 International Conference on, 2013, pp. 1-6.
- [4] R. A. Aoni, R. Ahmed, and S. Razzak, "Design and Simulation of Dual-Concentric-Core Photonic Crystal Fiber for Dispersion Compensation," in *CIOMP-OSA Summer Session on Optical Engineering, Design and Manufacturing*, 2013, p. Tu2.
- [5] J. Homola, "Present and future of surface plasmon resonance biosensors," *Anal. Bioanal. Chem.*, vol. 377, pp. 528-539, 2003.
- [6] A. Rifat, G. Mahdiraji, D. Chow, Y. Shee, R. Ahmed, and F. Adikan, "Photonic Crystal Fiber-Based Surface Plasmon Resonance Sensor with Selective Analyte Channels and Graphene-Silver Deposited Core," *Sensors*, vol. 15, pp. 11499-11510, 2015.
- [7] R. Jorgenson and S. Yee, "A fiber-optic chemical sensor based on surface plasmon resonance," *Sens. Actuators B Chem.*, vol. 12, pp. 213-220, 1993.
- [8] M. A. Schmidt, L. P. Sempere, H. K. Tyagi, C. G. Poulton, and P. S. J. Russell, "Waveguiding and plasmon resonances in two-

- dimensional photonic lattices of gold and silver nanowires," *Phys. Rev. B*, vol. 77, p. 033417, 2008.
- [9] J. N. Dash and R. Jha, "SPR Biosensor Based on Polymer PCF Coated With Conducting Metal Oxide," *IEEE Photon. Techn. L.*, vol. 26, pp. 595-598, 2014.
- [10] B. Shuai, L. Xia, and D. Liu, "Coexistence of positive and negative refractive index sensitivity in the liquid-core photonic crystal fiber based plasmonic sensor," *Opt. express*, vol. 20, pp. 25858-25866, 2012.
- [11] R. Jha and J. Dash, "Graphene Based Birefringent Photonic Crystal Fiber Sensor Using Surface Plasmon Resonance," *IEEE Photon. Techn. L.*, vol. 26, pp. 1092-1095, 2014.
- [12] P. J. Sazio, A. Amezcua-Correa, C. E. Finlayson, J. R. Hayes, T. J. Scheidemantel, N. F. Baril, et al., "Microstructured optical fibers as high-pressure microfluidic reactors," *Science*, vol. 311, pp. 1583-1586, 2006.
- [13] R. Otipiri, E. Akowuah, S. Haxha, H. Ademgil, F. AbdelMalek, and A. Aggoun, "A Novel birefringent photonic crystal fibre surface plasmon resonance biosensor," *IEEE Photonic J.*, vol. 6, No. 4, 2014.
- [14] A. A. Rifat, G. Amouzad Mahdiraji, Y. M. Sua, Y. G. Shee, R. Ahmed, D. M. Chow, et al., "Surface Plasmon Resonance Photonic Crystal Fiber Biosensor: A Practical Sensing Approach," *IEEE Photon. Techn. L.*, p. 1, 2015.
- [15] V. Kravets, R. Jalil, Y.-J. Kim, D. Ansell, D. Aznakayeva, B. Thackray, et al., "Graphene-protected copper and silver plasmonics," *Scientific reports*, vol. 4, 2014.
- [16] R. A. Aoni, R. Ahmed, M. M. Alam, and S. A. Razzak, "Optimum design of a nearly zero ultra-flattened dispersion with lower confinement loss photonic crystal fibers for communication systems," *Int. J. Sci. Eng. Res.*, vol. 4, pp. 1-4, 2013.